Sub-10-fs pulse generation from a blue laser-diode-pumped Ti:sapphire oscillator

Han Liu (刘 寒)[1], Geyang Wang (王阁阳)[1], Jianwang Jiang (蒋建旺)[1], Wenlong Tian (田文龙)[1], Dacheng Zhang (张大成)[1], Hainian Han (韩海年)[2], Shaobo Fang (方少波)[2], Jiangfeng Zhu (朱江峰)[1,*], and Zhiyi Wei (魏志义)[2]

[1]*School of Physics and Optoelectronic Engineering, Xidian University, Xi'an 710071, China*
[2]*Beijing National Laboratory for Condensed Matter Physics, Institute of Physics, Chinese Academy of Sciences, Beijing 100190, China*
**Corresponding author: jfzhu@xidian.edu.cn*

Received December 12, 2019; accepted April 16, 2020; posted online June 11, 2020

Pulses as short as 8.1 fs were generated from a blue laser-diode-pumped Kerr-lens mode-locked Ti:sapphire oscillator, with an average power of 27 mW and a repetition rate of 120.6 MHz. The full width at half-maximum exceeds 146 nm, benefitting from the dispersion management by a combination of a low-dispersion fused silica prism pair and a series of double-chirped mirrors. To the best of our knowledge, this is the first time to generate sub-10-fs pulses from a laser diode directly pumped Ti:sapphire oscillator.

Keywords: diode-pumped lasers; titanium; mode-locked lasers.
doi: 10.3788/COL202018.071402.

Ti:sapphire is an excellent and widely used gain medium in the near-infrared region due to its high thermal conductivity, broad absorption bandwidth, and large cross section of the stimulated emission. In 1991, the Kerr-lens mode-locking (KLM) phenomenon was firstly, to the best of our knowledge, discovered in a Ti:sapphire laser pumped by an argon-ion laser[1]. Various types of pump sources were used to pump Ti:sapphire lasers, including an argon-ion laser[1,2], frequency-doubled diode-pumped solid-state laser (DPSSL)[3], frequency-doubled fiber laser[4], and optically pumped semiconductor laser (OPSL)[5]. Although many of them have good beam quality and high brightness, these pump sources tend to be quite complicated and therefore very expensive. The laser diode (LD), on the other hand, with compact fabrication and simple packaging, can support high output power with stable performance at much lower cost[6,7]. With the development of GaN-based materials, high-brightness and high-power blue–green LDs have become increasingly mature, which also enables the development of LD directly pumped Ti:sapphire laser.

In 2009, a 452 nm LD directly pumped Ti:sapphire laser demonstrated by Roth *et al.* obtained continuous wave (CW) laser output[8]. Mode-locked Ti:sapphire lasers, directly pumped by blue–green LDs were reported later by different groups, based on either KLM or passive mode-locking using a semiconductor saturable absorber mirror (SESAM)[9–19]. In contrast to SESAM passive mode-locking, which is usually limited by the operable bandwidth, KLM can support larger bandwidth for mode-locking and, therefore, shorter pulse duration. So far, the shortest pulses reported were achieved by KMLabs Inc. from a blue LD-pumped KLM Ti:sapphire laser[13]. A single 3.1 W 465 nm LD was used as the pump, and pulses as short as 13 fs were generated from a prism-dispersion-managed oscillator. Further reduction of the pulse duration needs to manage the self-phase modulation (SPM) and residual high-order dispersions. Few-cycle pulses down to sub-10-fs can find important applications in spectroscopy[20], metrology[21], optical coherent tomography[22], optical frequency comb[23], etc. Till now, there is no report on sub-10-fs pulse generation directly from an LD-pumped Ti:sapphire oscillator.

In this Letter, we report sub-10-fs pulse generation from an LD directly pumped Ti:sapphire oscillator by fine management of the dispersion and SPM. Pulses as short as 8.1 fs were obtained with an average power of 27 mW and a repetition rate of 120.6 MHz. This is, to the best of our knowledge, the first demonstration on LD directly pumped Ti:sapphire lasers to deliver sub-10-fs pulses.

The experimental setup is schematically illustrated in Fig. 1. We used a 455 nm LD with a maximum power of 3.5 W as the pump source (Beijing Laserwave Opto-Electronics Technology Co. Ltd., Model LWBL455-3.5 W). The pump diode emits p polarized laser radiation (p:s = 100:1). The LD beam firstly passed through a beam shaping system consisting of an aspheric lens ($f_{L1} = 4$ mm) and two cylindrical lenses ($f_{L2} = -30$ mm and $f_{L3} = 300$ mm), after which the beam spot size was 8 mm and 3 mm in the horizontal and vertical directions, respectively. For the gain medium, a 3.5-mm-long, Brewster-cut Ti:sapphire crystal with 0.25% doping was mounted in a copper heat-sink, maintained at 20°C by a water cooling system. The single-pass absorption coefficient through the gain medium is 71% for the 455 nm LD, which is lower than that of the 532 nm laser (88%), primarily because the 455 nm wavelength deviates far from the Ti:sapphire absorption peak. For the laser cavity, the oscillator used a standard Z-fold cavity with astigmatism compensation. The output-coupler (OC) arm and the

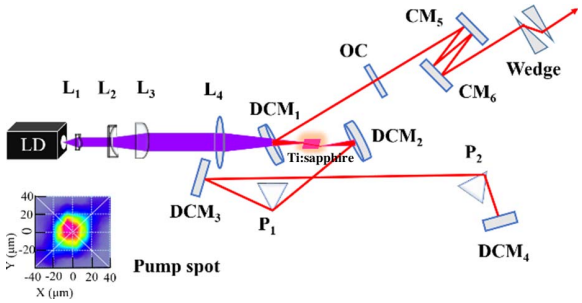

Fig. 1. Experimental setup of the blue LD-pumped Ti:sapphire oscillator. A 455 nm LD was used with a beam shaping system (L_1, L_2, and L_3) as the pump source. The lens L_4 focused the pump into a Ti:sapphire crystal, with the pump spot as shown in the inset. Curved double-chirped mirrors DCM_1 and DCM_2, flat double-chirped mirrors DCM_3 and DCM_4, output-coupling mirror OC, and prism pair P_1 and P_2 formed the laser cavity. Chirped mirrors CM_5 and CM_6 and a pair of wedges were used for extra-cavity dispersion compensation.

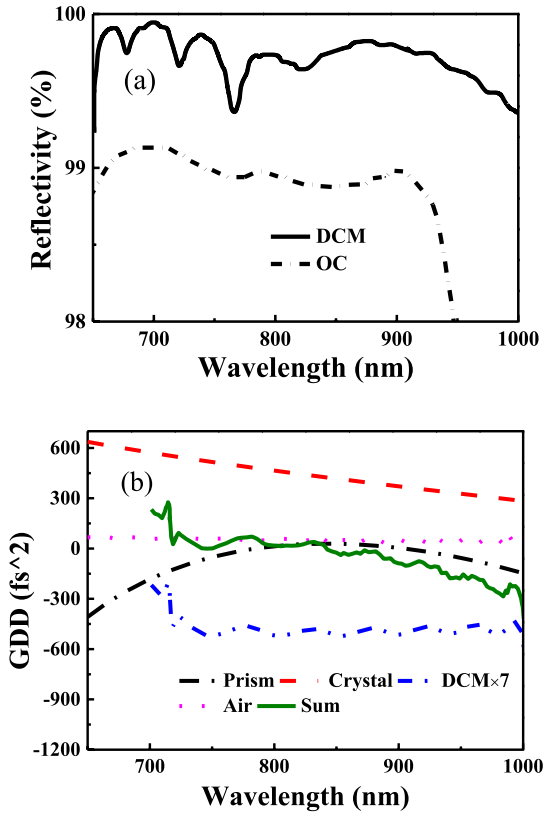

Fig. 2. (a) Reflectivity of the mirrors in the cavity. (b) Round-trip GDDs of the Ti:sapphire crystal, seven DCMs, prism pair, air, and their total sum.

dispersion-compensating arm (or prism arm) were 360 mm and 840 mm in length, respectively, corresponding to a repetition rate of 120.6 MHz. Two concave mirrors (double-chirped mirrors, DCM_1 and DCM_2) with radius of curvature (ROC) of 50 mm were used to increase the power intensity inside the crystal, where the waist radius of the cavity was about 22 μm. In order to achieve better spatial mode matching, the pump was focused to be $30\,\mu m \times 18\,\mu m$ by a spherical lens ($f_{L4} = 60$ mm). CW laser output of 65 mW could be obtained with a 1% OC when the pump power was 3.5 W.

DCMs and a pair of fused silica prisms were used to compensate for the positive chirp introduced by the Ti:sapphire crystal material, SPM, and the air along the optical path. The wavelength range with high reflectivity of the DCM ($R > 99.7\%$) was from 650 nm to 1000 nm, as shown in Fig. 2(a). The dispersion bandwidth of these DCMs was 720–1000 nm [Fig. 2(b), for seven DCMs in a round trip], which could provide a relatively flat negative group delay dispersion (GDD) of $-70\,fs^2$. By changing the insertion amount of the prism, we could have continuous adjustment of the net dispersion in the cavity. An OC as thin as 1 mm was selected to minimize the material dispersion with 1% transmission in the 660–920 nm range [Fig. 2(a)].

Figure 2(b) shows the total cavity round-trip GDD (green curve), taking into account the Ti:sapphire crystal, the prism pair with 380 mm separation, 2500 mm air, and seven reflections of the DCMs, where the GDD of the Ti:sapphire crystal per round trip was $+406\,fs^2$ at 800 nm, the GDD of the 2500 mm air was $+50\,fs^2$, and the total negative GDD by seven reflections on the DCMs was $-490\,fs^2$. Moreover, the third-order dispersion (TOD) of a 3.5-mm-long Ti:sapphire crystal per round trip was $+296\,fs^3$, and the 2500 mm air introduced extra $+25\,fs^3$ TOD. We continuously adjusted the prism insertion to obtain a net GDD and a TOD of approximately $-10\,fs^2$ and $-6\,fs^3$, respectively. We initiated soft-aperture KLM in the vertical direction by moving the P_1 prism. In this case, the average output power reduced to 27 mW.

A saddle-shaped mode-locking spectrum was recorded by a commercial optical spectrum analyzer showing the center wavelength at 800 nm with 146 nm full width at half-maximum (FWHM) bandwidth [Fig. 3(a)], which could support as short as 8.4 fs Fourier-transform-limited (FTL) $sech^2$-shaped pulses [inset in Fig. 3(a)]. We speculated that the sign of GDD changed around 800 nm, which may contribute to the middle dip in the saddle-shaped spectrum due to a worse condition for mode-locking near the center of the spectrum[24]. Such saddle-shaped spectrum is a benefit for seeding the Ti:sapphire amplifier, which may effectively reduce the gain narrowing effect. A pair of chirped mirrors (CM_5 and CM_6, with $-40\,fs^2$ GDD per bounce at 650–1000 nm) and a pair of wedges were used for chirp compensation outside the cavity. Though frequency-resolved optical gating (FROG) or self-referencing spectral phase interferometry for direct electric field reconstruction (SPIDER) methods could give more information for complete characterization of sub-10-fs pulses, the pulse energy in this case is only 0.25 nJ, which is difficult for carrying out FROG or SPIDER measurements, while the interferometric autocorrelation (IAC) is simple and acceptable for few-cycle pulses down to 5 fs[25,26]. As a result, we measured the pulse duration using IAC in the experiment. Figure 3(b) shows

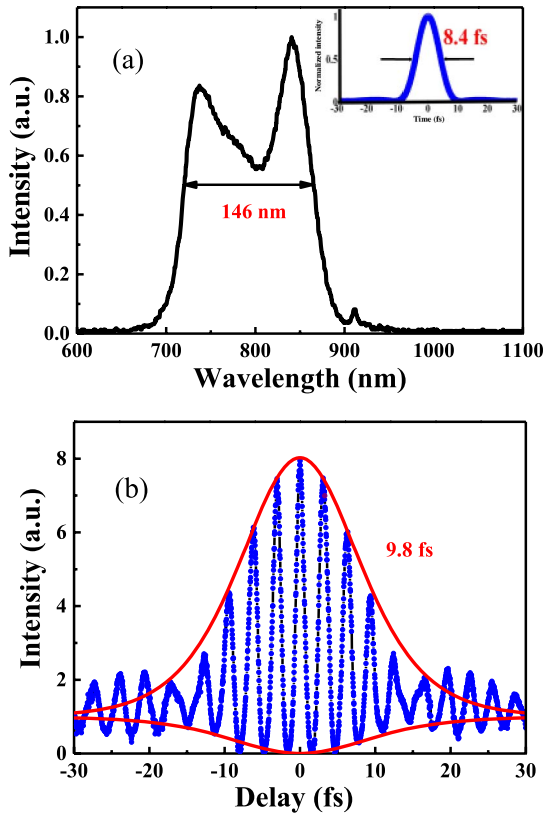

Fig. 3. Pulse profiles of the LD-pumped Ti:sapphire oscillator. (a) Mode-locking spectrum. Inset shows the FTL pulse in the time domain. (b) IAC trace of the pulse (blue curve), and an envelope of a theoretical sech^2 pulse of 9.8 fs (red curve).

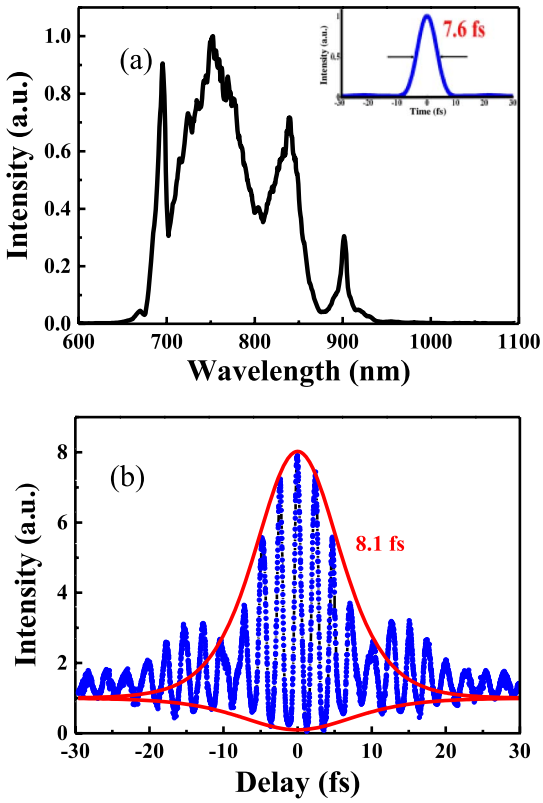

Fig. 4. Pulse profiles after adjusting the prism insertion. (a) Mode-locking spectrum. Inset shows the FTL pulse in the time domain. (b) IAC trace of the shortest pulse generated from the Ti:sapphire oscillator (blue curve) and theoretical IAC envelope of a sech^2 pulse of 8.1 fs (red curve).

the IAC trace of the pulses measured by an interferometric autocorrelator (Femtolasers GmbH). A sech^2 fit of the IAC trace yielded a pulse duration of 9.8 fs. The side lobes on both sides of the main IAC peak indicate uncompensated higher-order dispersions, which are common but difficult to eliminate in sub-10-fs pulses[24,27,28].

When the insertion amount of the P_2 prism increased, the signs of the intra-cavity net GDD and TOD shifted to positive, resulting in a broader mode-locking spectrum with multiple peaks, as shown in Fig. 4(a). The peaks of the spectrum are a result of the interaction of dispersion substructure and SPM in the laser crystal. However, the output power remained almost the same as before. This spectrum could support FTL sech^2-shaped pulses as short as 7.6 fs [inset of Fig. 4(a)]. Finally, 8.1 fs pulses were obtained, as shown in Fig. 4(b). The number of interference fringes was significantly reduced, while the side lobes in the IAC trace were more prominent than that in Fig. 3(b), which meant that the pulses contained more higher-order dispersion. When the prism insertion increased, the positive GDD and TOD increased correspondingly in the cavity, and the residual positive TOD would make the spectrum asymmetric, shifting the pulse central wavelength and producing dispersive waves[29,30].

In the case of a certain dispersion oscillation intensity, the saturation behavior of the KLM mechanism is critical to the final substructure in the spectrum[26]. Therefore, it is necessary to provide a stronger KLM action to suppress the modulation in the spectrum, so as to keep a flat spectrum phase and to better compress the pulses outside the cavity.

To check the status of mode-locking when the oscillator outputs the shortest pulses, radio-frequency (RF) spectra of the mode-locked laser were measured with an RF spectrum analyzer (Agilent E4407B) using a photo-detector with a 3 dB bandwidth of 1 GHz. Figure 5 shows a distinct signal-to-noise ratio as high as 63 dB of the fundamental beat at 120.6 MHz with a resolution bandwidth (RBW) of 1 kHz. The RF spectrum was clean, without side peaks or harmonics of the fundamental frequency. Harmonics modulation was not observed in the 1 GHz range with an RBW of 100 kHz (inset of Fig. 5).

The mode-locking operation was very stable with an output power of 27 mW under 3.5 W pump power. Even if the laser was exposed to the open air, the power remained stable with a power stability of 0.8% (RMS) over 3 h, as shown in Fig. 6.

In conclusion, we have generated sub-10-fs pulses directly from a blue LD-pumped Kerr-lens mode-locked Ti:sapphire oscillator by fine dispersion management inside and outside the laser cavity. The 9.8 fs pulses with 146 nm spectral bandwidth and 8.1 fs pulses with

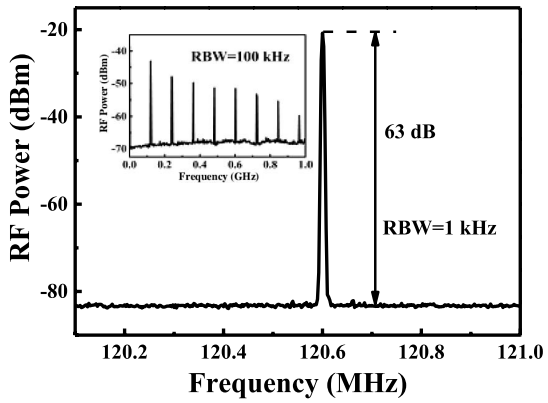

Fig. 5. RF spectra of the 8.1 fs Kerr-lens mode-locked Ti:sapphire laser, with an RBW of 1 kHz. The inset shows the RF spectrum in the 1 GHz range with a 100 kHz resolution.

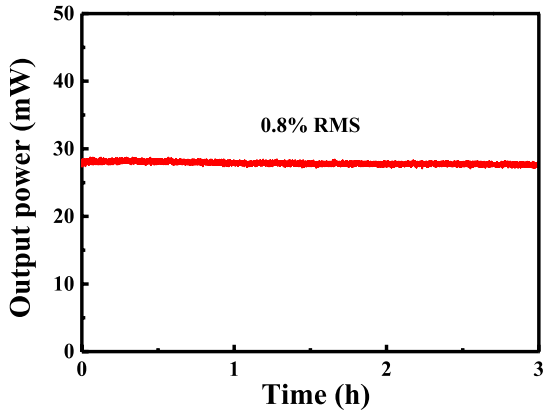

Fig. 6. Power stability of the single LD-pumped Kerr-lens mode-locked Ti:sapphire oscillator over 3 h.

mode-locking spectrum from 650 nm to 950 nm were obtained, respectively. Although wavelengths of 515–525 nm LDs are closer to the absorption peak of the Ti:sapphire crystal than that of 445–465 nm LDs with a higher pump efficiency, they are limited to ∼1 W in terms of the output power. Double-ended pumping with the blue LDs, a higher transmission OC, and the crystal with suitable length and absorption coefficient may have the chance to improve the laser output power[31]. Moreover, we would like to employ the 465 nm blue LD and a CaF_2 prism pair with lower higher-order dispersion to further reduce the pulse duration to the 5 fs regime.

This work was supported by the National Key R&D Program of China (No. 2016YFB0402105).

References

1. D. E. Spence, P. N. Kean, and W. Sibbett, Opt. Lett. **16**, 42 (1991).
2. A. Stingl, M. Lenzner, Ch. Spielmann, F. Krausz, and R. Szipöcs, Opt. Lett. **20**, 602 (1995).
3. R. Ell, U. Morgner, F. X. Kärtner, J. G. Fujimoto, E. P. Ippen, V. Scheuer, G. Angelow, T. Tschudi, M. J. Lederer, A. Boiko, and B. Luther-Davies, Opt. Lett. **26**, 373 (2001).
4. G. K. Samanta, S. C. Kumar, K. Devi, and M. E. Zadeh, Opt. Laser Eng. **50**, 215 (2012).
5. B. Resan, E. Coadou, S. Petersen, A. Thomas, P. Walther, R. Viselga, J. M. Heritier, J. Chilla, W. Tulloch, and A. Fry, Proc. SPIE **6871**, 687116 (2008).
6. X. Yan, S. Luo, B. Xu, H. Xu, Z. Cai, J. Li, H. Dong, L. Zhang, and Z. Luo, Chin. Opt. Lett. **16**, 020005 (2018).
7. Y. Zhang, Y. Yang, L. Zhang, D. Lu, M. Xu, Y. Hang, S. Yan, H. Yu, and H. Zhang, Chin. Opt. Lett. **17**, 071402 (2019).
8. P. W. Roth, A. J. Maclean, D. Burns, and A. J. Kemp, Opt. Lett. **34**, 3334 (2009).
9. C. G. Durfee, T. Storz, J. Garlick, S. Hill, J. A. Squier, M. Kirchner, G. Taft, K. Shea, H. Kapteyn, M. Murnane, and S. Backus, Opt. Express **20**, 13677 (2012).
10. S. Sawai, A. Hosaka, H. Kawauchi, K. Hirosawa, and F. Kannari, Appl. Phys. Express **7**, 022702 (2014).
11. K. Gürel, V. J. Wittwer, M. Hoffmann, C. J. Saraceno, S. Hakobyan, B. Resan, A. Rohrbacher, K. Weingarten, S. Schilt, and T. Südmeyer, Opt. Express **23**, 30043 (2015).
12. K. Gürel, V. J. Wittwer, S. Hakobyan, S. Schilt, and T. Südmeyer, Opt. Lett. **42**, 1035 (2017).
13. S. Bachus, M. Kirchner, C. Durfee, M. Murnane, and H. Kapteyn, Opt. Express **25**, 12469 (2017).
14. A. Rohrbacher, O. E. Olarte, V. Villamaina, P. Loza-Alvarez, and B. Resan, Opt. Express **25**, 10677 (2017).
15. R. Sawada, H. Tanaka, N. Sugiyama, and F. Kannari, Appl. Opt. **56**, 1654 (2017).
16. D. A. Kopylov, M. N. Esaulkov, I. I. Kuritsyn, A. O. Mavritskiy, B. E. Perminov, A. V. Konyashchenko, T. V. Murzina, and A. I. Maydykovskiy, Laser Phys. Lett. **15**, 045001 (2018).
17. J. C. E. Coyle, A. J. Kemp, J.-M. Hopkins, and A. A. Lagatsky, Opt. Express **26**, 6826 (2018).
18. N. Sugiyama, H. Tanaka, and F. Kannari, Jpn. J. Appl. Phys. **57**, 052701 (2018).
19. H. Liu, G. Wang, K. Yang, R. Kang, W. Tian, D. Zhang, J. Zhu, H. Han, and Z. Wei, Chin. Phys. B **28**, 094213 (2019).
20. M. Kreß, T. Löffler, M. D. Thomson, R. Dörner, H. Gimpel, K. Zrost, T. Ergler, R. Moshammer, U. Morgner, J. Ullrich, and H. G. Roskos, Nature Phys. **2**, 327 (2006).
21. J. Stenger, T. Binnewies, G. Wilpers, F. Riehle, H. R. Telle, J. K. Ranka, R. S. Windeler, and A. J. Stentz, Phys. Rev. A **63**, 021802 (2001).
22. J. G. Fujimoto, C. R. Acad. Sci. Paris Ser. **2**, 1099 (2001).
23. S. A. Diddams, J. Opt. Soc. Am. B **27**, B51 (2010).
24. I. P. Christov, M. M. Murnane, H. C. Kapteyn, J. Zhou, and C. Huang, Opt. Lett. **19**, 1465 (1994).
25. I. D. Jung, F. X. Kärtner, N. Matuschek, D. H. Sutter, F. Morier-Genoud, G. Zhang, and U. Keller, Opt. Lett. **22**, 1009 (1997).
26. U. Morgner, F. X. Kärtner, S. H. Cho, Y. Chen, H. A. Haus, J. G. Fujimoto, E. P. Ippen, V. Scheuer, G. Angelow, and T. Tschudi, Opt. Lett. **24**, 411 (1999).
27. A. Ge, B. Liu, W. Chen, H. Tian, Y. Song, L. Chai, and M. Hu, Chin. Opt. Lett. **17**, 041403 (2019).
28. J. Zhou, G. Taft, C. Huang, M. M. Murnane, and H C. Kapteyn, Opt. Lett. **19**, 1149 (1994).
29. T. Brabec and S. M. J. Kelly, Opt. Lett. **18**, 2002 (1993).
30. P. F. Curley, Ch. Spielmann, T. Brabec, F. Krausz, E. Wintner, and A. J. Schmidt, Opt. Lett. **18**, 54 (1993).
31. P. F. Moulton, J. G. Cederberg, K. T. Stevens, G. Foundos, M. Koselja, and J. Preclikova, Opt. Mater. Express **9**, 2131 (2019).